HHS Public Access

Author manuscript

Nat Neurosci. Author manuscript; available in PMC 2011 July 19.

Published in final edited form as:

Nat Neurosci. 2010 July ; 13(7): 822–824. doi:10.1038/nn.2570.

Target-selective GABAergic control of entorhinal cortex output

Csaba Varga[*], **Soo Yeun Lee**[*], and **Ivan Soltesz**

Department of Anatomy & Neurobiology, University of California, Irvine

Abstract

The medial entorhinal cortex (MEC) is a major center for spatial navigation and memory. We demonstrate that cannabinoid type-1 receptor-expressing GABAergic basket cells selectively innervate principal cells in layer II of the rat MEC that project outside the hippocampus, but avoid neighboring cells giving rise to the perforant pathway to the dentate gyrus. These results show that the organization of GABAergic microcircuits reflects the long-distance axonal targets of principal neurons.

Keywords

interneuron; cannabinoid; spatial navigation; grid cell; dentate gyrus; GABA

Layer II of the medial entorhinal cortex ($MEC_{layerII}$) is a key part of a distributed network for spatial navigation and memory processing[1–4], and it gives rise to the associational glutamatergic pathway known as the perforant path that terminates in the molecular layer of the dentate gyrus[5,6]. In neocortical and hippocampal networks, a major regulator of principal neurons is the cholecystokinin and cannabinoid type-1 receptor (CB1R) -expressing basket cells (CCKBCs)[7]. It is generally assumed that basket cells provide perisomatic inhibition to all principal neurons within a given layer. Here we demonstrate that in $MEC_{layerII}$, CCKBCs do not innervate all principal neurons equally, but they show strong preference for the principal cell class that projects extra-hippocampally, while avoiding those cells that are the origins of the perforant path. These results show that CCKBCs are specific in selecting principal cells based on their long-range axonal targets, indicating that local GABAergic microcircuits differentially participate in distinct information processing streams. Our experimental protocols (see Supplementary Methods) were approved by the Institutional Animal Care and Use Committee of the University of California, Irvine.

CCK-positive terminals surrounded the somata of some, but not all, presumed principal cells in $MEC_{layerII}$ (Fig. 1a). What determines which cells are targeted and which are avoided by CCKBCs? We aimed to identify cellular markers that may correlate with CCKBC

Correspondence: Csaba Varga, PhD, Anatomy & Neurobiology, University of California, Irvine, Irvine, CA 92697-1280, cvarga@uci.edu.

*These authors contributed equally to this work

Author Contribution statement: C.V., S.Y.L., and I.S. designed the research, C.V. and S.Y.L. performed research and analyzed data, and C.V., S.Y.L., and I.S. wrote the paper.

innervations. We found that there are two major, non-overlapping cell groups in $MEC_{layerII}$ in similar abundance, that could be distinguished based on their immunoreactivity to reelin[8] or calbindin[9] (Fig. 1b; % of immunolabeled cells: calbindin$^+$: 44.2±2.2%, reelin$^+$: 53±2.6%; calbindin$^+$ and reelin$^+$: 2.8±1.1%; n=1152 cells; n=3 animals; note that reelin$^+$ and calbindin$^+$ cells were intermixed in layer II and frequently adjacent to each other; Fig. 1c,d). Surprisingly, when the retrograde tracer biotinylated dextrane amine (BDA) was injected into the ipsilateral dentate gyrus, the majority of BDA-labeled cells were reelin-positive in $MEC_{layerII}$ (Fig. 1c; % of BDA-labeled cells that were reelin$^+$: 98.5±0.5; n=1135 cells; n=3 animals; note that similar results were obtained with fluorogold tracer; data not shown). These results demonstrated that only the reelin-expressing principal cells project to the dentate gyrus, therefore, the perforant pathway originates from some but not all principal cells in $MEC_{layerII}$. Critically, the CCKBCs avoided the reelin-positive cells and formed perisomatic inhibitory inputs with a high degree of specificity onto the calbindin-positive cell population in $MEC_{layerII}$ (Fig. 1d; CCKBC terminals were visualized using vesicular glutamate transporter-3 (VGLUT3) as an alternative marker, because it allows sharper visualization of CCK$^+$/CB1R$^+$ axon terminals[10]; see also Supplementary Methods and Supplementary Fig. 1; number of VGLUT3$^+$ putative axon terminals per 1mm of somatic membrane: calbindin$^+$ cells: 95.6±10.4; reelin$^+$ cells: 8.6±1.8; n=329 terminals; n=3 animals; P=0.0001). Electron microscopy demonstrated that the VGLUT3$^+$ axon terminals formed synaptic contacts (Supplementary Fig. 2; synapses from VGLUT3$^+$ terminals in $MEC_{layerII}$ on somata: 50.1±5.8%, with the rest on dendrites; no spines were targeted; n=195 synapses; n=3 animals).

The specificity of the CCKBC innervation pattern demonstrated above was tested in electrophysiological experiments. CCKBCs express CB1Rs on their axon terminals[7], and activation of CB1Rs by postsynaptically released ligands can depress GABA-release through a short-term plasticity mechanism known as depolarization-induced suppression of inhibition (DSI)[11]. In agreement with the anatomical data in Fig. 1, patch clamp recordings from $MEC_{layerII}$ cells followed by post-hoc immunocytochemistry showed that those neurons that exhibited DSI were immunoreactive for calbindin, whereas the reelin-positive cells on average showed no significant DSI (Fig. 2a; % of charge transfer following a 500ms depolarizing pulse to 0mV with respect to the pre-pulse period, in the presence of carbachol: calbindin$^+$: 40.1±8.0%, n=13 cells; reelin$^+$: 106±10.6%, n=12 cells; P=0.0001; carbachol was used to boost sIPSC frequency and DSI[11]). DSI was abolished in the presence of the CB1R antagonist AM251 (calbindin$^+$ cells: 98.2±11.4%, n=3), and the difference in DSI was also present without carbachol (calbindin$^+$ cells: 51.6±0.1%, n=3; reelin$^+$: 118.2±0.2%, n=3; P=0.03). Furthermore, paired recordings showed that the DSI sensitive perisomatic inputs formed functional synapses and originated from local interneurons (Supplementary Fig. 3; DSI: 31.1±0.09%, with respect to the pre-pulse unitary IPSC amplitude, with failures included; n=3 pairs; additional CCK$^+$ inputs to MEC may originate from outside the entorhinal cortex[12]). Note also that the calbindin$^+$ and reelin$^+$ cells also differed in their intrinsic electrophysiological properties (Supplementary Table 1).

Do the calbindin-expressing $MEC_{layerII}$ neurons targeted by the CCKBCs possess any characteristic long-distance axonal projection pattern? The results in Fig. 1 showed that the calbindin cells do not project to the dentate gyrus. When we injected the retrograde tracer

fluorogold into the hippocampal commissure/fimbria-fornix region, the majority of fluorogold-labeled cells were calbindin^{+} in $MEC_{layerII}$ (% of fluorogold-labeled cells that were calbindin^{+}: 88.9±8.0; reelin^{+}: 2.2±1.9; n=1231 cells; P<0.001; n=3 animals), demonstrating that these neurons project extra-hippocampally. Because our tracer injections showed bilateral labeling in $MEC_{layerII}$ and previous studies have indicated the presence of commissural connections between the entorhinal cortices traveling through the dorsal hippocampal commissure[13], we tested the hypothesis that calbindin-expressing cells in $MEC_{layerII}$ send their axons to the contralateral entorhinal cortex. Unilateral injection of retrograde tracers into the MEC confirmed this prediction (Fig. 2b; % of fluorogold-containing cells retrogradely labeled from the contralateral MEC that were calbindin^{+}: 93.3±4.5; reelin^{+}: 1.6±1.4; n=1354 cells; P<0.001; n=4 animals).

Taken together, the data in this paper show that CCKBCs do not indiscriminately innervate potential glutamatergic principal cells within the same cell layer, but that they choose their synaptic targets based on the long-distance axonal projection patterns of the postsynaptic cells, revealing a new level of specificity of the CCKBC inhibitory system[5,14]. Therefore, similarly to what has been demonstrated recently for glutamatergic neocortical synaptic connections[15], GABAergic microcircuits are also differentially involved in distinct information processing streams originating from a single layer. In addition, our results identified cellular markers (reelin and calbindin) that specifically label two distinct principal cell groups within $MEC_{layerII}$ with differential projection targets. Unit recordings from behaving animals have revealed the existence of two distinct cell populations in $MEC_{layerII}$, the grid cells[1] and the border cells[2], and future studies will need to determine how these in vivo electrophysiological cell types correspond to the two differentially projecting $MEC_{layerII}$ principal cell classes described in this paper, and how they are modulated by segregated GABAergic microcircuits in vivo.

Supplementary Material

Refer to Web version on PubMed Central for supplementary material.

Acknowledgments

We thank R. Zhu and M. Cid for technical assistance, and I. Sears-Kraxberger and H.S. Keirstead for their generous support with electron microscopy. This work was supported by the US National Institutes of Health grant NS35915 (to I.S.) and the American Epilepsy Society (to S.Y.L.).

References

1. Hafting T, Fyhn M, Molden S, Moser MB, Moser EI. Nature. 2005; 436:801–806. [PubMed: 15965463]
2. Solstad T, Boccara CN, Kropff E, Moser MB, Moser EI. Science. 2008; 322:1865–1868. [PubMed: 19095945]
3. Mizuseki K, Sirota A, Pastalkova E, Buzsáki G. Neuron. 2009; 64:267–280. [PubMed: 19874793]
4. Peng PY, et al. Neuron. 2009; 63:230–243. [PubMed: 19640481]
5. Steward O, Scoville SA. J Comp Neurol. 1976; 169:347–370. [PubMed: 972204]
6. van Strien NM, Cappaert NL, Witter MP. Nat Rev Neurosci. 2009; 10:272–282. [PubMed: 19300446]
7. Freund TF, Katona I. Neuron. 2007; 56:33–42. [PubMed: 17920013]

8. Chin J, et al. J Neurosci. 2007; 27:2727–2733. [PubMed: 17360894]
9. Fujimaru Y, Kosaka T. Neurosci Res. 1996; 24:329–343. [PubMed: 8861103]
10. Somogyi J, et al. Eur J Neurosci. 2004; 19:552–569. [PubMed: 14984406]
11. Kano M, Ohno-Shosaku T, Hashimotodani Y, Uchigashima M, Watanabe M. Physiol Rev. 2009; 89:309–380. [PubMed: 19126760]
12. Jinno S, et al. J Neurosci. 2007; 27:8790–8804. [PubMed: 17699661]
13. Adelmann G, Deller T, Frotscher M. Anat Embryol. 1996; 193:481–493. [PubMed: 8729966]
14. Bodor AL, et al. J Neurosci. 2005; 25:6845–6856. [PubMed: 16033894]
15. Brown SP, Hestrin S. Nature. 2009; 457:1133–1136. [PubMed: 19151698]

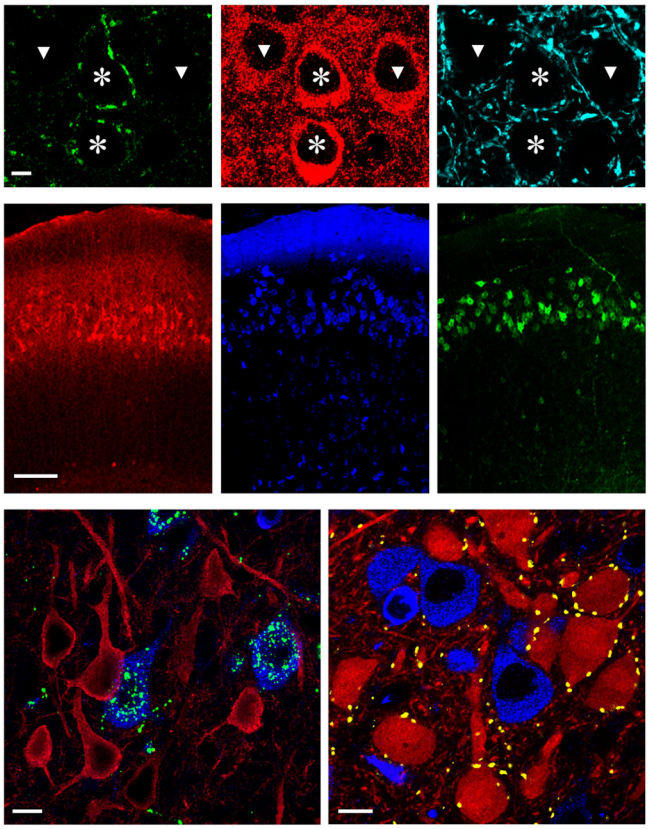

Figure 1. Cell type-specific targeting of principal cells by CCK-positive basket cells in $MEC_{layerII}$

(**a**) CCK-immunopositive axon terminals (left panel) selectively surround the somata of some (asterisks) but not all (triangles) principal cells in $MEC_{layerII}$ (principal cells were visualized by GluR2/3 immunopositivity, see Supplementary Methods; middle panel). In contrast, axons from parvalbumin (PV) positive basket cells[7] (right panel) surround the perisomatic region of most principal cells. (**b**) $MEC_{layerII}$ cells exhibit immunoreactivity for reelin (blue) or calbindin (red), and were retrogradely labeled (green) following BDA injections into the ipsilateral dentate gyrus. Note that most $reelin^+$ cells are non-GABAergic[8] and control experiments showed that only 2.4±0.4% of $MEC_{layerII}$ $calbindin^+$ cells were GABA-immunopositive (data not shown). (**c**) The $reelin^+$ and $calbindin^+$ cells formed two largely non-overlapping populations, and only the $reelin^+$ cells were retrogradely labeled (intracellular green deposits) from the dentate gyrus. (**d**) $VGLUT3^+$ terminals (yellow, used as an alternative marker for CCK/CB1R-expressing terminals[10]) can be found predominantly on the somatic membranes of the $calbindin^+$ (red) cells in $MEC_{layerII}$. Calb: Calbindin. Scale bars: a,c,d: 10μm; b:100μm.

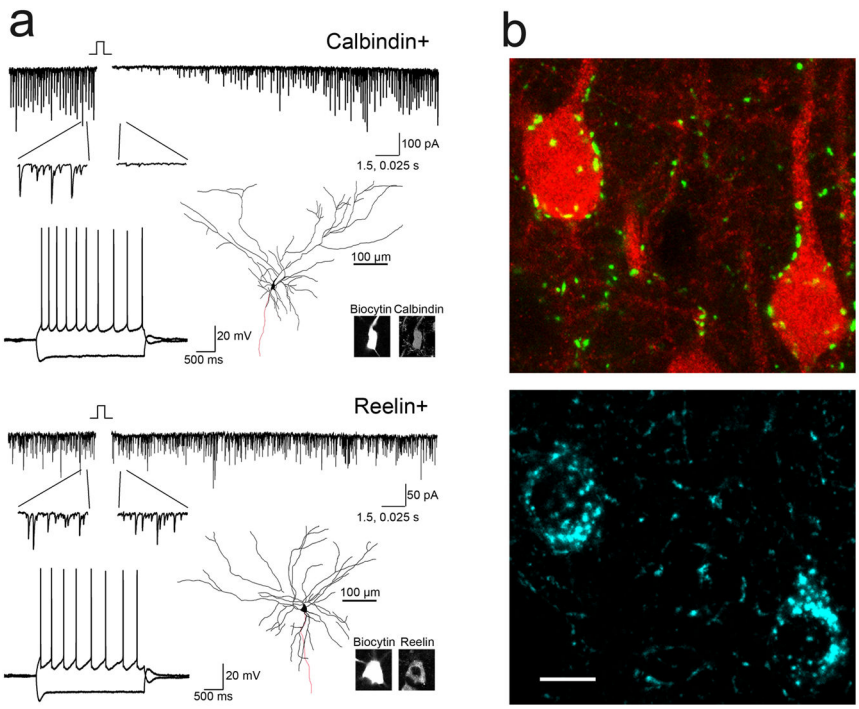

Figure 2. Calbindin$^+$ MEC$_{layerII}$ cells express DSI and project to the contralateral entorhinal cortex

(**a**) Example traces (top) illustrating sIPSCs from a calbindin$^+$ or a reelin$^+$ cell from MEC$_{layerII}$; note the depression of the sIPSCs (DSI) following the injection of a depolarizing current pulse (500ms to 0mV from −60mV) only in the calbindin$^+$ cell (inset). Bottom right panels show the reconstruction and post-hoc immunocytochemical identification of the recorded cells (red: axon); the bottom left traces illustrate the characteristic firing patterns and hyperpolarizing responses after intracellular current injections. Note that, because the intrapipette solutions differed for the recordings of sIPSCs/DSI and the intrinsic firing properties (see Supplementary Methods), the current clamp and voltage clamp (DSI) traces were from different cells. **(b)** After injection of the retrograde tracer fluorogold into the contralateral entorhinal cortex, calbindin$^+$ cells were labeled in MEC$_{layerII}$ that were surrounded by VGLUT3$^+$ terminals (scale bar: 10µm).